Features of Plasma Interaction with Tungsten Brush Surfaces under Transient Plasma Loads Simulating ITER Divertor Conditions

I.E. Garkusha[1], V.A. Makhlaj[1], S. Herashchenko[1], B. Bazylev[2], M.J. Sadowski[3], E. Skladnik-Sadowska[3],

[1]*Institute of Plasma Physics, NSC KIPT, Ukraine*

[2]*Karlsruhe Institute of Technology (KIT), IHM, Germany*

[3] *National Centre for Nuclear Research, Poland*

NATIONAL SCIENCE CENTER "KHARKOV INSTITUTE OF PHYSICS AND TECHNOLOGY"
INSTITUTE OF PLASMA PHYSICS

Outline

- Introduction
- Numerical codes
- Experimental Setup
  - QSPA Kh-50- quasi-stationary plasma accelerator
  - Exposed targets
- ELM-like plasma loads resulting in surface melting
  - Features of energy transfer to the surface
  - Droplets and solid dust ejection from W surfaces
  - Dynamics of melt losses
- Summary

NATIONAL SCIENCE CENTER "KHARKOV INSTITUTE OF PHYSICS AND TECHNOLOGY"
INSTITUTE OF PLASMA PHYSICS

Motivation

Tungsten in ITER Divertor and possible choice for DEMO

W:
- -sputtering yield
- -sputtering threshold energies
- -thermal conductivity
- -melting temperature
- -tritium retention
  - - brittleness
  - - high DBTT
  - - melt
  - - high Z

- **Material erosion restricts the divertor lifetime**
- **Plasma contamination by impurities (high Z)**
- **Dust (tritiated, radioactive and chemically reactive)**

Disruption:

$Q = (10\text{-}100)\ MJ/m^2$;
$t = (1\text{-}10)$ ms

Type I ELM in ITER:

- **up to 10^3 ELMs/ITER pulse**
- **Million ELMs for operation cycle**
- **$Q = \sim 1\ MJ/m^2$**
- **t =0.1-0.5 ms**

NATIONAL SCIENCE CENTER "KHARKOV INSTITUTE OF PHYSICS AND TECHNOLOGY"
INSTITUTE OF PLASMA PHYSICS

Motivation

Macroscopic mechanisms of W erosion rather than microscopic ones:

- **-Brittle destruction (cracks, debris and dust)**
- **-Melt losses (motion, droplets)**
- **-Material modification (changed properties)**
- **-Synergetic effects**

Simulators of transient loads: e-beams, PG, QSPA, PSI devices

Cost effective, flexible, faster results.

Comparison of results is important!

Insufficient database from existing machines. Only few tokamaks have experience with W.
ITER loads (especially for disruption) will exceed the available loads in experimental devices . Resulting damage effects from million ELMS?

Castellation: to reduce the influence of electric currents induced on the metallic surfaces during the reactor operation as well as to minimize the thermal stresses and resulting tungsten erosion caused by the formation of macro crack meshes

Castellated edges of macro-brush armour elements of ITER divertor can be a source of molten/solid dust particles which are injected into the plasma

Numerical Codes for Simulation of Disruptions and ELMs

Codes	PEGASUS-3D	MEMOS PHERMOBRID	FOREV	TOKES
Tasks	1) brittle destruction in grain Graphite & CFCs 2) heat conductivity in W, 3) thermostress & tungsten surface cracking 4) Dust productions	1) melting processes &re--solidification 2) brittle destruction in CFC & graphite 3) droplets	1) C influx, erosion & contamination 2) Evaporation and shielding effects	1) multi-fluid transport 2) plasma both in the bulk and the edge region
Dimention Equations	3D fluid Thero-mechanical, transient	2D/3D Navier-Stocks in shallow water approx. transient	2D fluid, transient	2D fluid Braginskii, steady-state

Validation against experimental results
Predictions for ITER and DEMO

S. Pestchanyi et al. Fusion Sci. and Techn., 2014
Y.Igitkhanov, B.Bazylev. IEEE Transactions on Plasma Science, 2014

The code MEMOS for numerical simulations of surface damage

MEMOS is developed for flat and macro-brush targets

Shallow water approximation (L>>h, parabolic approximation for $V_x(z)$),

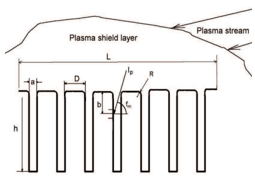

Cross-section of macro-brush target and the plasma shield layer above it. Schematic representation

Driving forces, caused the melt motion:
- gradient of plasma pressure
- gradient of surface tension
- JxB force; current flowing into the armour
- tangential friction force of dumped plasma

Physical processes taken into account:
1. heating, melting, melt front propagation
2. Heat transport across the fluid&solid
3. Evaporation from surface
4. Melt motion by driving forces
5. Thermo-emission current (Richardson expression)

Energy deposition:
Monte-Carlo calculation for e-beams heat loads
FOREV-2D output data for plasma heat loads

3D version of the code MEMOS was tested and is available now

NATIONAL SCIENCE CENTER "KHARKOV INSTITUTE OF PHYSICS AND TECHNOLOGY"
INSTITUTE OF PLASMA PHYSICS

QSPA Kh-50 device

W~ 4 MJ
U_c=15kV
I_d~0.7 MA
τ=0.25 ms
ρ_W= 1-30 MJ/m^2
E~0.5-0.9 keV
B_{ext}≤0.7T

Vacuum chamber:
L=10m
∅=1.5m

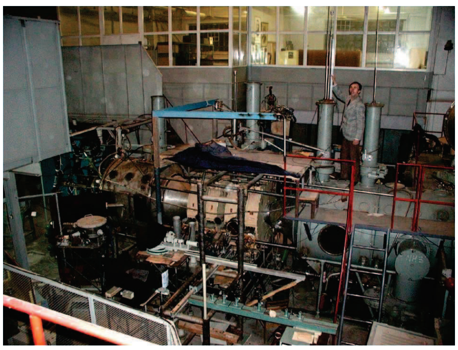

QSPA plasma parameters are relevant to the ITER high heat loads (typical for disruptions and ELMs) to the divertor plates.

NATIONAL SCIENCE CENTER "KHARKOV INSTITUTE OF PHYSICS AND TECHNOLOGY"
INSTITUTE OF PLASMA PHYSICS

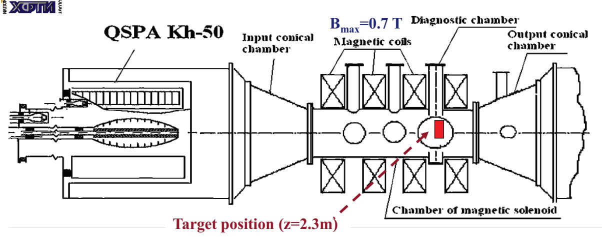

Rogowski coils, voltage dividers, electric and magnetic probes, piezodetectors, bolometer, movable calorimeters, high-speed cameras in different modifications, time-of-fly energy analyzer. Spectroscopy: Stark broadening of the H_β and self-absorption H_α spectral lines, autocollimation interferometer with view area of 200 mm in diameter.

The velocity of different parts of the plasma stream: time-dependent modulation of radiation using the slit scanning and registration by a high-speed camera, Doppler shift of spectral lines. Electron temperature : ratio of spectral lines intensities, analysis of contours.

NATIONAL SCIENCE CENTER "KHARKOV INSTITUTE OF PHYSICS AND TECHNOLOGY"
INSTITUTE OF PLASMA PHYSICS

QSPA Plasma Parameters in ELM simulation Regimes

Parameters	ELM 1 no melting	**ELM 2 melting**	ELM 3 evaporation
Plasma stream energy density [MJ/m²]	0.9-1.0	1.2-1.5	2.4-2.5
Target Heat Load [MJ/m²]	**0.45**	**Varied 0.6-0.9**	**1.1**
Plasma load duration [ms]	0.25	**0.25**	0.25
Half-height width [ms]	0.1-0.12	**0.17**	0.1-0.14
Shape of heat signal	triangular	**bell**	triangular
Maximal plasma pressure [bar]	4.8	**3.2**	4.5
Average plasma density [10^{16} cm^{-3}]	1.5-2.5	**0.5-0.7**	0.2-0.3
Plasma stream diameter [cm]	12-14	**18**	16

Features of plasma energy transfer
Normal exposure

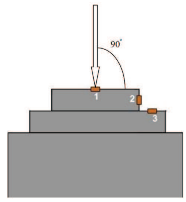

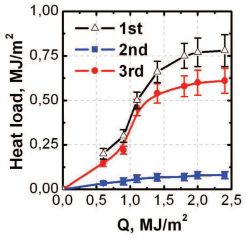

Heat load to different areas of target surfaces vs. the energy density of impacting plasma stream

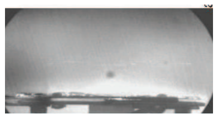

Image of plasma stream interaction with the target.

Plasma layer is created near exposed surface. This layer of cold plasma is responsible for decreasing part of incident plasma energy which is delivered to the surface.

Plasma-surface interaction: inclined impact

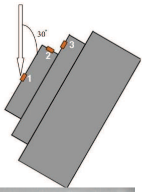

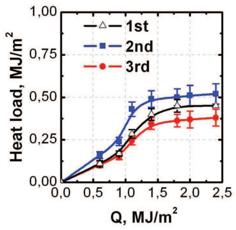

Heat load to the target surfaces vs. the energy density of impacting plasma stream

Image of plasma stream interaction with inclined target

For inclined surface irradiation the radial distribution of energy density is non-symmetric. The thickness of the shielding layer (width of luminous area in front of targets) is the smallest at the upper edge of the sample (forwarded to the plasma stream). This layer of cold plasma is responsible for decreasing part of incident plasma energy which is delivered to the surface.

Targets design and experimental conditions

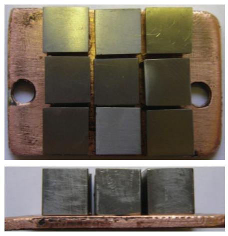

Titanium castellated target
The Ti cube size – 1 cm. The width of the gaps between the cubes ≈ 1 mm.
q = 0,75 MJ/m²

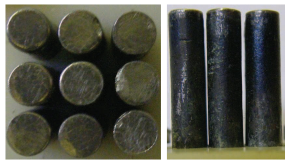

Tungsten brush target
W cylinder diameter – 5 mm, height – 2 cm. The min gap between the cylinders – 1 mm.
q ≈ 0,9 MJ/m²

Ti - to enhance the dynamics of the melt and to achieve the recognizable and measurable effects for smaller number of plasma pulses as well as separate cracks influence and to make clear the analysis of different possible mechanisms of the surface relief development

Normal plasma exposure

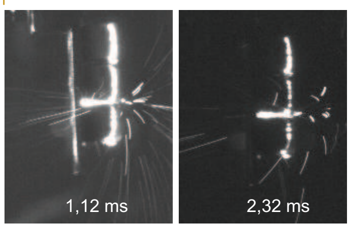

High speed imaging of PSI (35th pulse)

The sharp edges of cubes became locally overheated

Particles are emitted toward to the incident plasma flow, which may indicate the development of Kelvin-Helmholtz instability at the interface between the molten layer and moved plasma

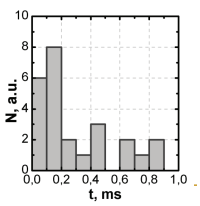

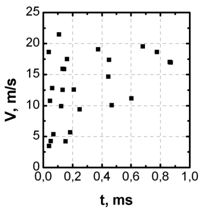

CCD imaging of PSI (74th pulse)

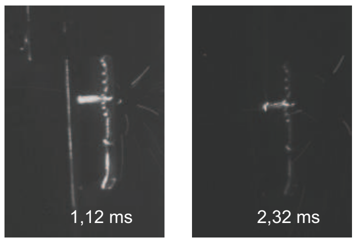

The particles begin to be emitted from the surface almost immediately after the start of the interaction.

The average delay time is 10-40 μs which is in reasonable consistent with estimates of the time of formation of the molten layer.

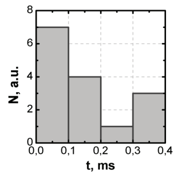

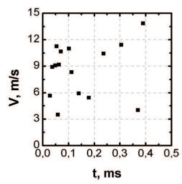

Number of emitted droplets and their velocity on the start time of the plasma-surface interaction.

Inclined plasma exposure

CCD imaging of PSI (30th pulse)

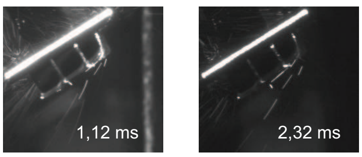

Intense overheating of the upper upstream part of the target is observed with the formation of outgrowth from shifted material to the neighborhood areas.

This re-solidified material mountain is the predominant region from which most of the observed particles are emitted.

Droplets are flying along the plasma flow.

Particles with the highest velocities start at earlier time instances in the range of 0.2 – 0.4 ms from the beginning of plasma surface interaction

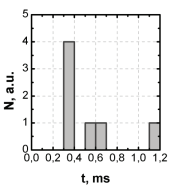

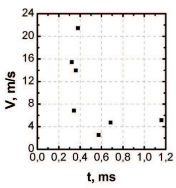

CCD imaging of PSI (41th pulse)

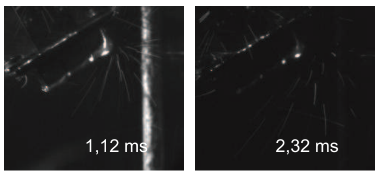

The number of ejected droplets increases

After 40 pulses an intense emission of particles is recorded from the shifted material outgrowth at the front of the castellated structure.

Droplets are flying toward and along the plasma flow.

The velocity for majority of the particles is in the range of 10 – 15 m/s

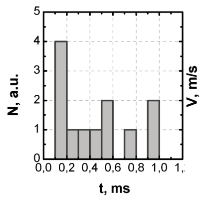

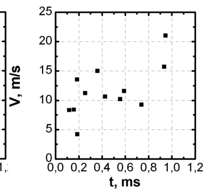

Amount of ejected particles v.s. number of plasma pulses

Normal exposure | Inclined target

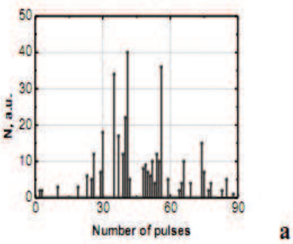

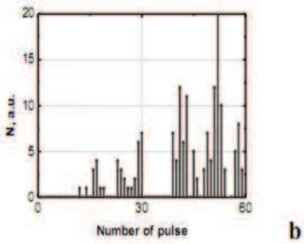

Emission of droplets begins only after a certain number of plasma pulses when the mountain of shifted molten material is developed on the edges of castellated structure

Melt motion and bridges formation on the edge of castellated structure

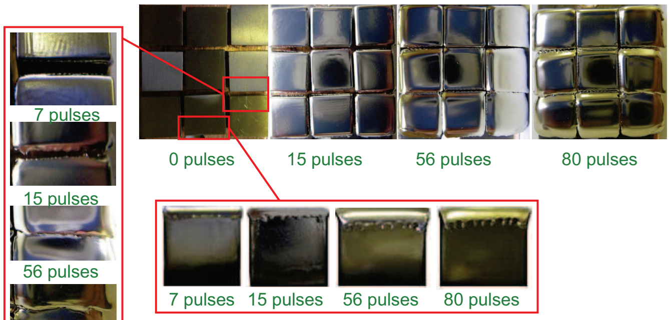

Mountains from the displaced material are formed not only on the outer perimeter, but also at the internal borders of the cubes

Correlation between formation of the bridges through the slits of castellated target and ejection of particles

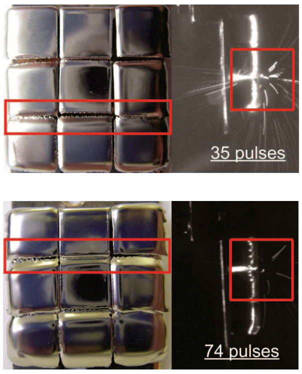

Melt motion leads to formation of mountains on the edges of macrobrush units and resolidified bridges through the gaps between them.

The droplets ejection begins only after the definite number of plasma pulses from the edges of the tiles and due to destruction of bridges between the fragments of construction.

The gaps filling by melt layer after a large number of pulses.

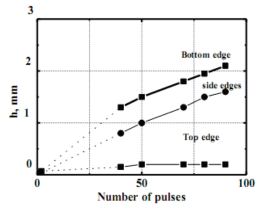

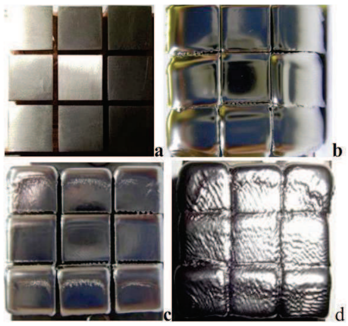

initial (a), normal (b) plasma exposure with 30 plasma pulses of 0.75 MJ/m2, inclined plasma exposure with 30 plasma pulses of 0.75 MJ/m2 (c) and 80 plasma pulses of 1 MJ/m2 (d).

Plasma irradiation of macrobrush tungsten target

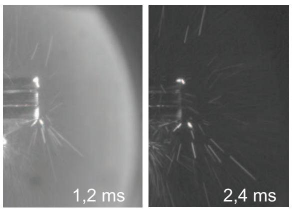

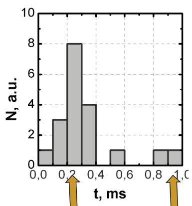

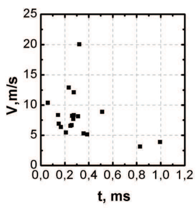

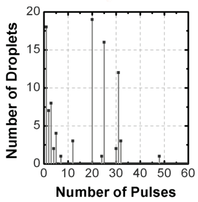

CCD imaging of tungsten exposures

Liquid droplets are ejected before 0.15 ms

Solid particles and liquid droplets – in the time interval of 0.15-0.2 ms

Most of emitted particles – solid dust – ejected after 0.2 ms

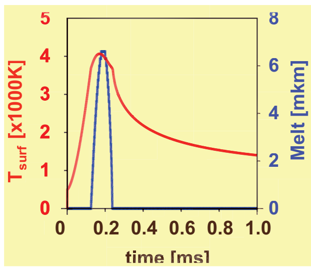

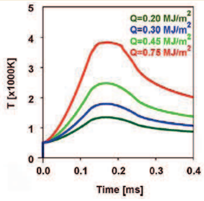

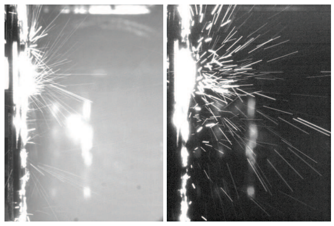

Time dependences for the surface temperature and the melt layer depth simulating the QSPA Kh-50 shot with energy density of 0.75 MJ/m2. The melt layer totally re-solidifies 0.23-025 ms after the heating start.

Comparison of target surfaces after different number of plasma impacts

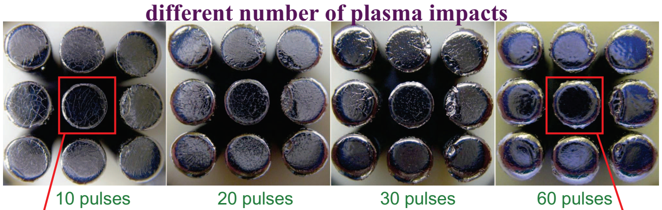

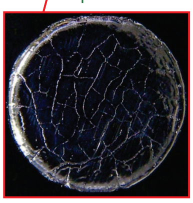

Initially the cracks develop on tungsten surface and solid particles ejection is observed

The cracks are filling by molten metal with increasing pulse number and number of ejected solid particles decreases

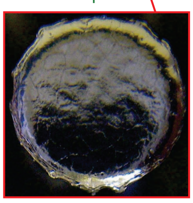

Kelvin-Helmholtz instability of the melt layer

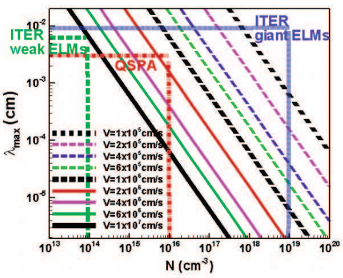

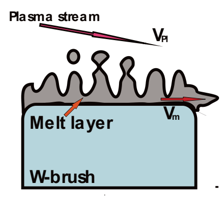

Droplet erosion:

Simulation of K-H Instability wavelengths

Dependence of the wave length of the KH wave with maximum growth rate on plasma density for different plasma velocities along the surface

Kelvin-Helmholtz instability of the melt layer

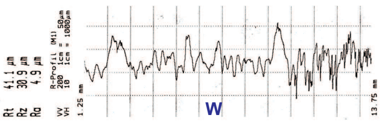

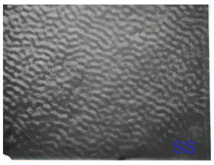

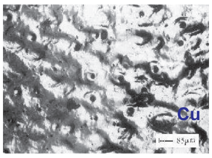

Wavy structures

Capillary waves

$$\omega = kv[\rho_{melt}/(\rho+\rho_{melt})], \quad \gamma = \frac{2\rho_{melt}v^3}{3\alpha}\sqrt{\frac{\rho_{melt}}{3\rho}}$$

$$k_{max} = \frac{2\rho_{melt}v^2}{3\alpha} \quad \lambda_{max} = \frac{3\pi\alpha}{\rho_{melt}v^2}$$

Tungsten: $\omega \approx 3\ 10^3$ c^{-1}, $\gamma \approx 10^6$ c^{-1}, **λ=50-90 µm**

λ_{Cu}~ 150 µm, λ_{Ti}~ 450 µm

Droplet erosion:

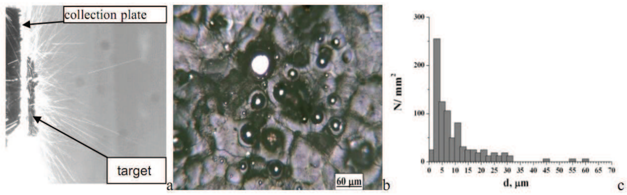

Picture of the plasma surface interaction (a), collected particles(b) and size distribution (c) of particles re-deposited upon the tungsten surface exposed to plasma pulses of 0.9 MJ/m^2.

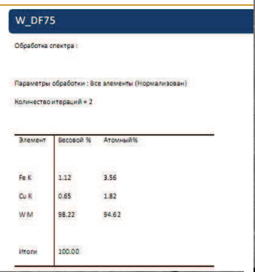

W_DF75

Обработка спектра :

Параметры обработки : Все элементы (Нормализован)

Количество итераций = 2

Элемент	Весовой %	Атомный%
Fe K	1.12	3.56
Cu K	0.65	1.82
W M	98.22	94.62
Итого	100.00	

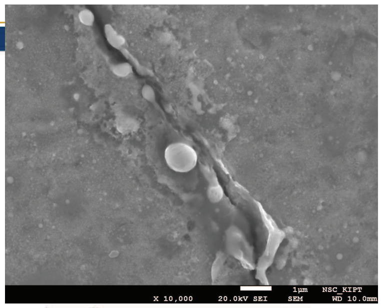

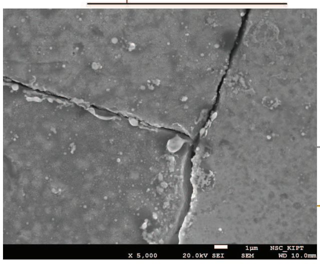

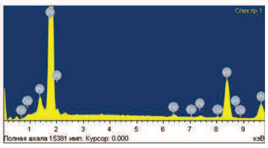

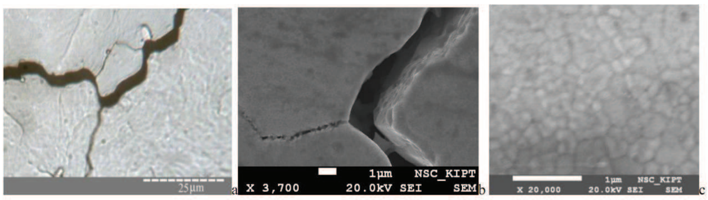

Sources of dust in different size scales:

Bifurcation of primary cracks

Microcracks along the grain boundaries (grain losses)

Bridges through the intergranular cracks

Cellular nanostructures due to surface modification

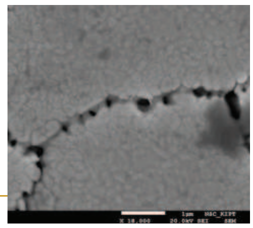

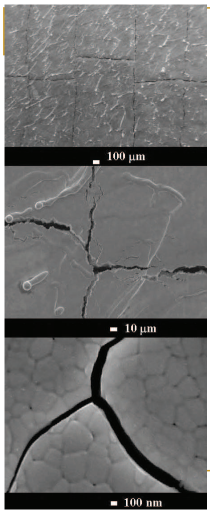

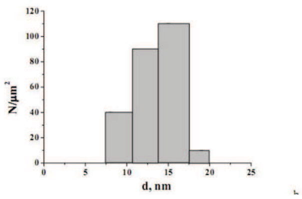

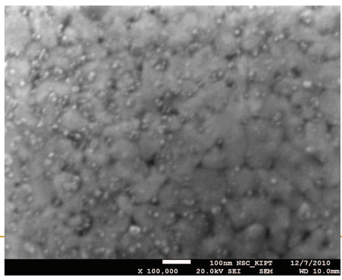

Summary

Melt dynamics at the structure edges, droplet splashing and molten bridges through the slits are main processes in macroscopic erosion of castellated surface structures

Melt accumulation at the edges. Emission of the droplets has a threshold character and the cyclical nature, i.e. it begins only after a certain number of irradiating pulses when the mountain of shifted molten material is developed on the edges of castellated structure

The obtained experimental results on dynamics of splashing in castellated geometry and droplets characterization are going to be used for further validation of the MEMOS numerical code

Dust dominates after pulse end. Most of particles ejected in solid state even for exposures with strong melting

Different sources of dust: bifurcation of major cracks, fine cracks along the grains, re-solidified micro-bridges through the cracks, material modification.

Thank you

for your attention!